RSC Advances

ROYAL SOCIETY OF CHEMISTRY

www.rsc.org/advances

Journal Name

ARTICLE

Preparation of alumina-coated graphite for thermally conductive and electrically insulating epoxy composites

Received 00th January 20xx,
Accepted 00th January 20xx

DOI: 10.1039/x0xx00000x

www.rsc.org/

Dahang Tang, Juqiao Su, Qi Yang*, Miqiu Kong, Zhongguo Zhao, Yajiang Huang, Xia Liao and Ying Liu

Herein, highly thermally conductive and insulating epoxy composites were reported. Firstly uniform alumina-coated graphite flakes were successfully prepared by a two-step coating method of chemical precipitation with the aid of sodium dodecyl sulfonate (SDS) surfactant using an inorganic precursor (aluminum nitrate) as the starting material. Then the alumina-coated graphite particle was incorporated into epoxy resin. The thermal conductivity value of epoxy/alumina-coated graphite composite shows a significant increase from 0.22 W/mK (neat epoxy) to 0.64 W/mK by factor of approximate 3 at the filler loading of 18.4%. Moreover, due to the presence of the alumina nanolayers coating on graphite surface, epoxy/alumina-coated graphite composites could retain high electrical volume resistivity of $>10^{10}$ Ω cm up to high filler contents, which was much higher than that of epoxy/graphite composites ($<10^{5}$ Ω cm) at the same filler loadings. And they still could be regarded as insulators.

Introduction

As a trend for developing denser and more miniature integrated circuits is highlighted, efficient thermal dissipation has caused increasing attention in the microelectronic applications.[1-3] Polymers such as epoxy resin are considered as promising thermal interface materials for the applications in electrically insulating fields in large scale, due to their light weight, low cost, ease of processing, good dimensional stability and excellent dielectric properties.[4, 5] Unfortunately, the low thermal conductivities (0.2-0.5 W/mK) of polymers present a major bottleneck in modern high packing and power-density devices.[6] Therefore, at present, in order to enhance the thermal conductivity, the incorporation of highly thermally conductive fillers into polymers is being considered by most researchers.

According to numerous studies in recent years, highly thermally conductive and insulating fillers, such as boron nitride,[7-9] aluminum nitride[10-12] and silicon nitride,[13, 14] etc., are commonly utilized to produce thermally conductive and electrically insulating composites to meet the stringent requirements for electrical insulation and high thermal conductivity in dielectric fields. But their high cost limits their commercial use.[15] Hence recently, extremely high intrinsic thermal conductivities of representative carbon materials, carbon nanotubes (CNTs)[6, 16] and graphene[17, 18] in the range of ~3000-3500 W/mK, have made them promising candidates for the preparations of thermally conductive and insulating polymeric composites as long as the filler contents are below the electrical percolation threshold.[15, 19] However, in fact, the low value of percolation threshold for CNTs or graphene (< 1 vol.%) cannot lead to a substantial improvement of thermal conductivity for polymer in most cases.[20, 21] Additionally, the poor dispersion of CNTs or graphene in polymer resins, in turn, sacrifices the enhancement of thermal conductivity.[3, 22]

Micro flake-graphite is considered as one of the most suitable fillers for the preparation of thermally conductive polymer composites because of its high thermal conductivity, low coefficient of thermal expansion, low cost, light weight, and flake shape in favor of the formation of thermally conductive chains.[1, 3, 23] Nevertheless, like CNTs and graphene, the excellent electrical properties of graphite particles could also cause some adverse influences on the insulating properties of polymers, which would depress their applications in dielectric areas. Thus, how to increase the thermal conductivity of polymer while maintaining its good insulating property with the introduction of carbon fillers at the same time becomes a crucial issue. In order to solve the problem mentioned above, carbon fillers coated by insulating inorganic layers were synthesized and added to polymers. Cui *et al.*[24, 25] fisrtly reported the incorporation of CNTs coated by silica through a sol-gel method into epoxy resin could improve the thermal conductivity of epoxy as well as retaining its high electrical resistivity. Shim *et al.*[3, 26] and Noma *et al.*[15] studied that the addition of silica-coated graphite into thermoplastic resins had few adverse effects on the electrically insulating properties because the silica coatings could prohibit the formation of a graphite electrically conductive network. Moreover, similar results were obtained for the polymer composites with carbon fillers coated by alumina (Al_2O_3) or boethmite (AlOOH) inorganic nanoparticles separately.[27-30] In summary, the precursors of the coating layers used in previous reports, such as tetra ethyl oxysilane (TEOS)[15, 21] and alkoxide metal (aluminum isopropoxide and aluminum tri-sec-butoxide),[27, 30] are almost organic materials. However, in fact, besides the organic precursors, owing to their much lower costs and better water-solubility, inorganic acid salts,

like aluminum nitrate ($(Al(NO_3)_3 \cdot 9H_2O)$) and aluminum chloride could be well utilized as the precursors of coatings as well.[31, 32]

In the present study, we tried to cover the surface of graphite with alumina nanoparticles by a simple liquid-phase chemical precipitation method with aluminum nitrate as the coating precursor. And the optimum synthesis condition for the uniform alumina coatings on graphite surface was demonstrated through the characterization methods of SEM, TEM, TGA and XPS. As a consequence, the introduction of alumina-coated graphite fillers into the epoxy resin not only significantly enhanced the thermal conductivity, but also retained the high electrical volume resistivity of the polymer matrix. To our best knowledge, few researches, if any, about the issue that thermally conductive and insulated epoxy composite based on graphite formed by means of an inorganic nanolayer (Al_2O_3) coating onto the graphite surface with an inorganic precursor ($Al(NO_3)_3 \cdot 9H_2O$) as the starting material have been reported.

Experimental

Materials

The diglycidyl ether of bisphenol-A resin, NPEL-128, from Nanya Plastic Co., Ltd, Taiwan, with an epoxide equivalent weight of 184-190 g equiv.$^{-1}$, was used in our study with curing agent of 4,4'-diamino diphenylmethane (DDM, Shandong Xiya Reagent Research Center, China). Flake graphite particle with diameter of about 30 μm was provided from Qingdao Chengyang graphite Co., Ltd. (Shandong, China). Surfactants of cetylpyridinium chloride (CPC) and sodium dodecyl sulfonate (SDS) were purchased from Beijing J&K Scientific Co., Ltd. And the chemical structure of the two kinds of surfactants is shown in Fig.1. $Al(NO_3)_3 \cdot 9H_2O$ and sodium hydroxide (NaOH) were supplied by Chengdu Kelong Chemical Co. Anhydrous ethanol used without further purification was offered by Chengdu Changlian Chemical Reagent Co.

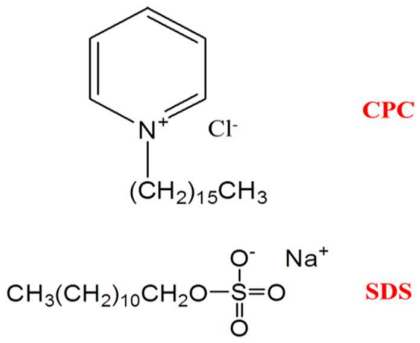

Fig. 1 Chemical structure of two kinds of surfactants, CPC and SDS in this work.

Synthesis of Al_2O_3-coated graphite particles

About 15 g graphite particles and various amounts of surfactant were dispersed in 500 ml distilled water with sonication energy of 150 W for 30 min, followed by vigorous mechanical agitation for another 2 h at 80 °C to obtain a stable and homogeneous suspension. Subsequently, appropriate amount of the alumina precursor, $Al(NO_3)_3 \cdot 9H_2O$, and NaOH solution were slowly added to the suspension simultaneously, to make the pH value remain at 6-7. Then the reaction was kept for 4 h under stirring again. After that, the graphite was isolated by centrifuged, filtration and washed with ethanol several times to obtain the product, aluminum hydroxide ($Al(OH)_3$) coated graphite ($Al(OH)_3$-graphite). Finally, the dried $Al(OH)_3$-graphite particles were calcined to undergo further decomposition at 550 °C for 3.5 h in quartz tube furnace to obtain Al_2O_3-coated graphite (Al_2O_3-graphite) fillers.[31, 33, 34] In this experiment, the amounts of each material were selected as variables. And the experimental conditions are shown in Table 1. What should be mentioned here is that the coating way of sample 6 is different from other six samples, which means the amount of alumina precursor was averaged into two parts to incorporate to the suspension. One part was added to the solution for first coating to obtain $Al(OH)_3$-graphite particles, followed by a second coating with other part of $Al(NO_3)_3 \cdot 9H_2O$. For the sake of understanding, this is named for two-step coating method distinguished from one-step coating method for other six samples. And the detailed synthesis process of Al_2O_3-graphite is shown in Fig.2. For a comparison, neat alumina particle was also produced without graphite in solution.

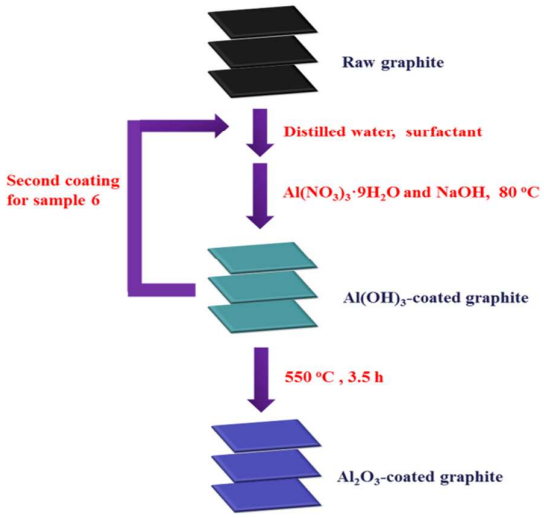

Fig. 2 Schematic representation of preparation process of graphite coated by Al_2O_3.

Preparation of epoxy composites

Typical epoxy/Al_2O_3-graphite composites were prepared as follows. Firstly, a desired amount of Al_2O_3-graphite fillers and epoxy resin were ultrasonically dispersed with 150 W in appropriate amount of ethanol for 15 min. Then, the solution was put into an oil pan for over 3 h with mechanical stirring to remove the ethanol entirely at 90 °C. Afterwards, the temperature was increased to 105 °C and the solution was degased for 30 min to remove bubbles before the curing agent was added. Subsequently, DDM, 39% weight fraction of epoxy, was introduced into the mixture under vigorous mechanical stirring, and the solution was degased for 20 min again until no obvious bubble could be noticed. Finally, the mixture was poured

Table 1 Experimental conditions for Al_2O_3 coating on graphite.

Sample	Graphite /g	Distilled water /ml	$Al(NO_3)_3 \cdot 9H_2O$ /g	NaOH /g	CPC /g	SDS /g
1	15	500	7.5	2.36	0	0
2	15	500	7.5	2.36	0.65	0
3	15	500	7.5	2.36	0	0.65
4	15	500	22.5	7.08	0	0.65
5	15	500	45	14.16	0	0.65
6	15	500	22.5	7.08	0	0.65
			22.5	7.08	0	0.65
7	15	500	45	14.16	0	1.3

onto the preheated polytetrafluoroethylene (PTFE) mold (at 130 ^oC) and cured at 130 ^oC for 4 h in an oven. Control samples of neat epoxy resin, epoxy/graphite, and epoxy/Al_2O_3 composites were also fabricated by using the same preparation conditions.

Characterization

The gold coated surfaces of alumina-coated or uncoated graphite and microstructure of epoxy composites samples, which were cryogenically fractured in liquid nitrogen, were observed using scanning electron microscopy (SEM; JEOL SJM-5900VL) with an operating voltage of 20 kV. Transmission electron microscopic (TEM) investigations were conducted using a Tecnai G2F20 S-TWIN (FEI Company, USA) instrument electron microscope set at 200 kV, and the samples were prepared for the TEM measurements by one drop casting on a lacey copper grid, with the solvent (ethanol) being evaporated under vacuum at room temperature. Thermogravimetric analysis (TGA) of the fillers with weight of 5~10 mg was conducted using an STA 449C (NETZSCH Company, Germany) instrument with a heating rate of 10 ^oC/min from room temperature to 1300 ^oC under an air atmosphere. X-ray photoelectron spectra (XPS) measurements were performed on an XSAM800 (Kratos Company, UK) instrument, to trace the variations in surface composition between raw graphite and Al_2O_3-coated graphite particles. The thermal conductivity of sample prepared in cylindrical shape of 30 mm in diameter and 2 mm in thickness, was measured by the standard model of hot disk thermal analyzer (Hot Disk, Uppsala, Sweden), which in this work is not just the in-plane or through-plane direction, but a comprehensive value of all directions. And the senor supplied a heat pulse of 0.02-0.03 W for 5-10 s to the samples. The electrical resistance of epoxy composites was measured with Keithley 6487 electrometer (Tektronix, USA). For a good contact, silver paint was applied to both ends of the sample. The volume resistivity (ρ) was calculated with the following equation:

$$\boldsymbol{\rho} = \frac{\boldsymbol{R \times S}}{\boldsymbol{L}} \qquad (1)$$

where *R, S* and *L* are the resistance, cross section area and length of the sample respectively. In addition, for the thermal conductivity and electrical resistance measurements, three specimens were tested and averaged for each group of specimens.

Results and Discussion

Morphological study

The morphology of raw graphite and Al_2O_3-graphite synthesized with different conditions was characterized using SEM, as depicted in Fig.3-5. Fig.3 shows that there exist no obvious changes between the surface morphology of raw graphite and that of graphite after coating reaction without surfactant, which suggests that alumina particles did not grow on the graphite surface. And the same result suits for the sample 2 after coating reaction with CPC. However, as compared with the smooth and clear surface of raw graphite, the surface of sample 3 coated in the presence of SDS surfactant is rough with the depositions of sponge-like alumina attached to the graphite surface.[35] This phenomenon indicates the deposition reaction with the aid of SDS, an anionic surfactant, could induce heterogeneous nucleation of $Al(OH)_3$ particles on the surface of graphite. On the contrary, homogeneous nucleation not on graphite surface is predominant in the solution with CPC, a cationic surfactant, resulting in the growth of uncoated free nanoparticles in the reaction medium.[36] A satisfactory explanation for this result can be obtained by considering the Derjaquin-Landau-Verwey-Overbeek theory.[15, 37] According to the theory, the total potential energy including Van der Waals forces and electrostatic potentials plays an important role in the process of particle dispersion and coagulation. When two different particles get close to each other and their energy is high enough to overcome the potential energy barrier, these particles can bind to each other.[15] In this study, SDS or CPC surfactant changed the surface charge of graphite from neutral to negatively or positively charged state, respectively. As a result, when $Al(NO_3)_3 \cdot 9H_2O$ was added to the solution, the formation of strong electrostatic interaction between negative graphite and Al^{3+} ions lowered the energy barrier between alumina precursor and graphite particles, facilitating the deposition of aluminum hydroxide on the surface of graphite. Then the nucleus subsequently enlarged to bigger particles or a shell, which transformed to alumina via calcination at 550 ^oC for 3.5 h.[15, 31, 38, 39] Based on above analysis, a

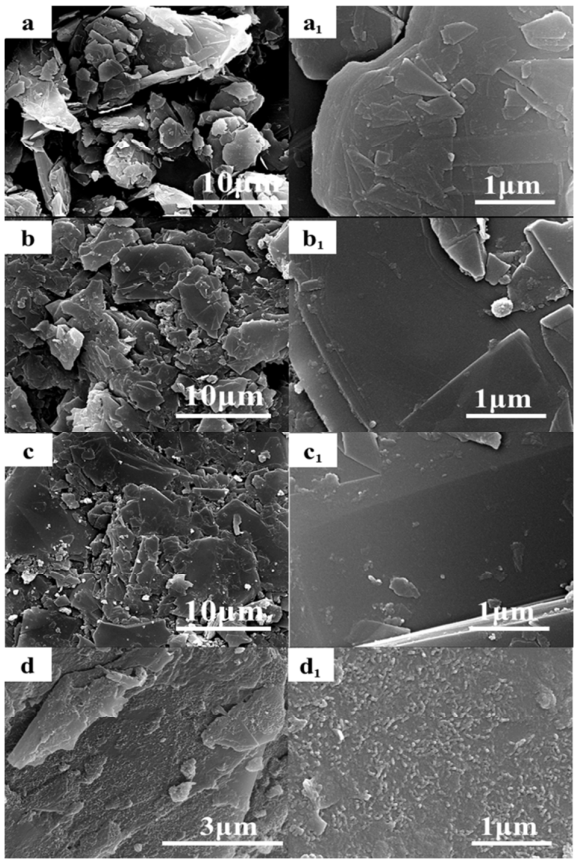

Fig. 3 SEM images of surface morphology of raw graphite (a and a_1), sample 1 (b and b_1), 2 (c and c_1), and 3 (d and d_1).

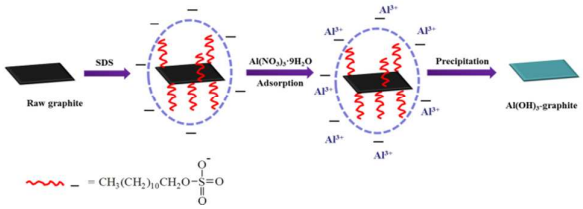

Fig. 4 Schematic representation of the synthesis of graphite coated by $Al(OH)_3$.

simulation scheme is proposed to illustrate the whole process for the preparation of $Al(OH)_3$-coated graphite particle in Fig.4.

As discussed above, alumina coatings attached on graphite surface could be formed with the assistance of SDS surfactant. To determine the optimum conditions for the alumina nanoparticles coating on graphite, coating reactions with SDS as a function of alumina precursor amounts were conducted. And the differences of surface morphology between sample 3, 4, 5, 6 and 7 are shown in Fig.5. It is seen that clear uncoated parts (shown in the red dashed-line box) of the surface of sample 3 exist anywhere in Fig.5a-a_1, which is attributed to the low content of alumina precursor. In comparison with sample 3, Fig.5b-b_1 shows that the proportion of alumina coverage on graphite surface of sample 4 is significantly enhanced due to the increase of alumina precursor by factor of 3. Previous studies exhibi-

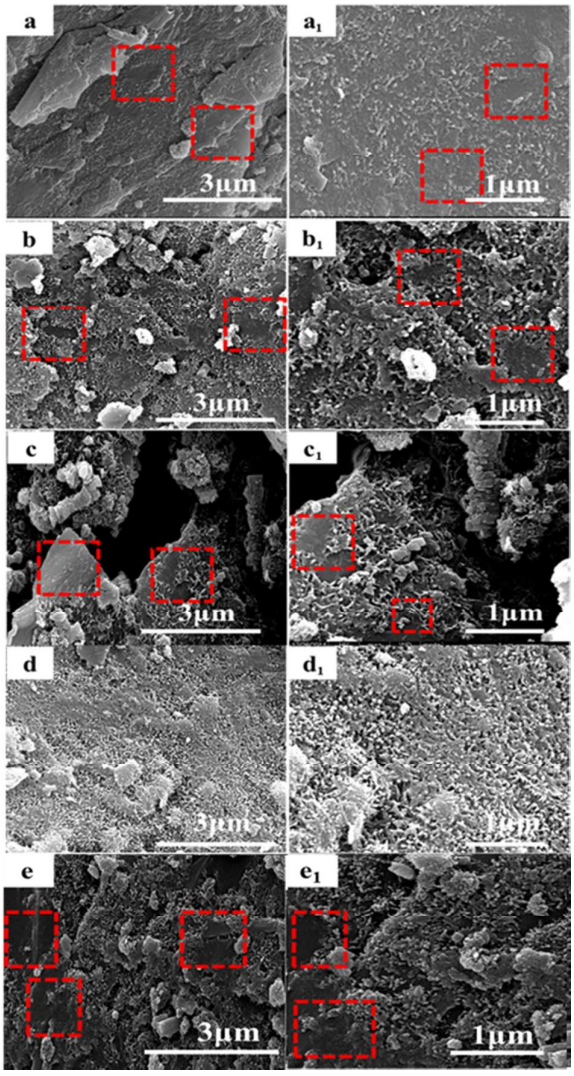

Fig. 5 SEM images of surface morphology of sample 3 (a and a_1), 4 (b and b_1), 5 (c and c_1), 6 (d and d_1), and 7 (e and e_1).

ted that uniform coating coverage of insulating material on graphite surface was necessary for maintaining the electrically insulating properties of polymer when that coated filler is introduced into it.[3, 25, 27, 36] Thus, the existence of some clear uncoated places on the surface of sample 4 may lead to some adverse effect on the insulating properties of polymer.

In addition, for the sample 5, 6 and 7 with the same mass of alumina precursor, the surface morphology exhibits obvious variations, which is ascribed to the different coating methods. Of course, sufficient amount of $Al(NO_3)_3 \cdot 9H_2O$ is essential for uniform coverage of alumina on graphite surface, whereas ultrahigh concentration of alumina precursor in solution would lead to the formation of homogeneously nucleated free $Al(OH)_3$ particles in the reaction medium, resulting in a decrease in the amount of alumina attached on graphite surface.[3, 27] That is why the proportion of alumina coverage shows no obvious increase for sample 5 as compared to sample 4. In contrary, uniform alumina coatings are observed on the surface of sample 6. This phenomenon could be

explained by considering the following reason. After the first coating with the half amount of the total alumina precursor, most of the graphite surface is coated with $Al(OH)_3$ particles, which would be the active sites for the growth of new hetero-nucleated $Al(OH)_3$ during the second coating process, inducing a thicker and more uniform coating coverage.[3, 40] In order to further confirm that the two-step coating method is the main reason for better coating effect of sample 6, sample 7 was prepared. Fig.5e-e_1 shows some uncoated parts of graphite surface still exit, which indicates the increase of the amount of SDS surfactant could not induce an improvement on the coating effect. To summarize, these morphological results guarantee that the two-step coating method is effective to make alumina nanoparticles uniformly attached on the graphite surface.

Fig.6 represents the TEM images of raw graphite and Al_2O_3-graphite (sample 6) powders, which shows that an alumina layer was formed, homogeneously coating the graphite surface with needle nanoparticles in Fig.6b (compared with the smooth uncovered pristine graphite shown in Fig. 6a).[21, 38] Furthermore, Fig.6b_1 reveals the thickness of alumina layer is approximately 60.32 nm.

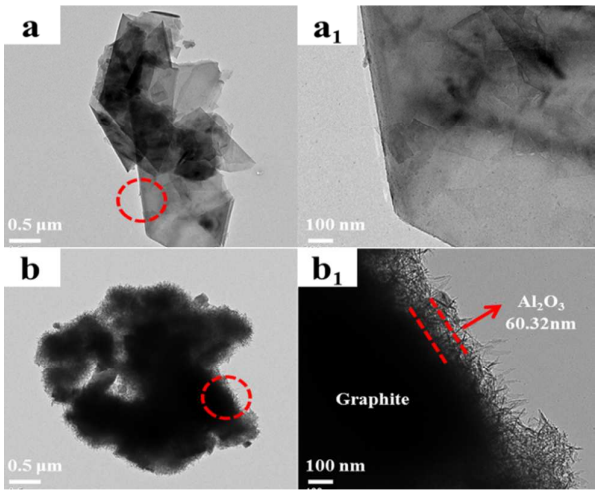

Fig. 6 TEM images of raw graphite (a and a_1) and Al_2O_3-graphite (b and b_1).

TG-analysis

TGA was utilized to evaluate the thermal stabilities of raw graphite and Al_2O_3-graphite powders and to determine the amount of alumina nanoparticles on graphite surface. Fig.7 shows the TGA thermograms of raw graphite, sample 3, sample 4 and sample 6 separately. It is indicated that about 4% residue was obtained above 1000 °C for raw graphite due to the inorganic impurities contained in graphite.[34] And the weights of the residues for the three alumina-coated graphite particles increase gradually (sample 3 is 8.3%, sample 4 is 18.28%, and sample 6 is 30.2%), suggesting that the amounts of alumina coating on the graphite surface enhance considerably, which also agrees well with the proportion of alumina coverage observed in SEM images (Fig.5). In addition, the inset in Fig.7 depicts that the alumina coatings on the surface of sample 6 cause a significant increase in the onset of weight loss relative to the thermal oxidative decomposition of carbon and a slower decompos-

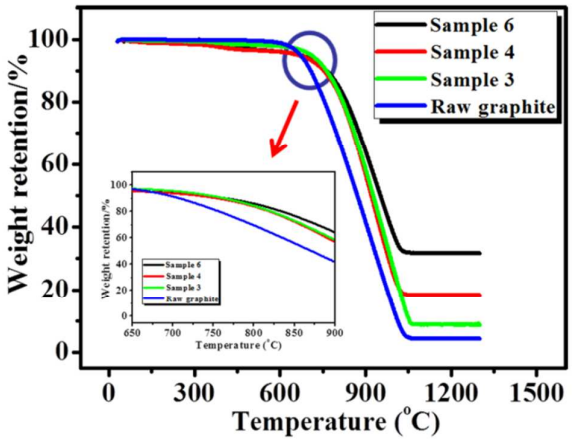

Fig. 7 TGA thermograms of raw graphite, sample 3 sample 4 and sample 6 under air atmosphere from room temperature to 1300 °C.

ition rate in comparison with that of raw graphite. Moreover, a slight higher decomposition temperature is also shown compared with the other two alumina-coated graphite powders. These results indicate that the coated alumina layer on graphite surface acts as a protective layer to prevent the oxidative degradation of the graphite, leading to a better thermal stability.[27] Based on the aforementioned findings, sample 6 was selected as the most suitable coated filler for insulating epoxy composites in the next study in terms of its uniform alumina coatings with higher coverage.

XPS-analysis

XPS is an effective method to characterize the variations in surface composition of graphite and Al_2O_3-graphite filler after the coating reaction. Fig.8 shows the spectra of raw graphite, Al_2O_3 and Al_2O_3-graphite separately. In comparison with the spectra of raw graphite, two new peaks in the spectra of Al_2O_3-graphite in Fig.8a, corresponding to Al 2p and Al 2s, respectively, indicate alumina was successfully attached on the graphite surface. The oxygen-containing functional groups can be identified by deconvoluting the C1s and O1s spectra of graphite and Al_2O_3-graphite, and the peaks at 284.5, 285.8, 287.1 and 288.4 eV correspond to C=C, C-C, hydroxyl (C-OH), carbonyl (C=O) and carboxylate (O-C=O) moieties separately, as shown in Fig.8b.[3, 21, 41] In addition, a peak at about 291.7 eV, is attributed to π–π* excitation owing to the restoration of delocalized π conjugation of the graphene sheets in graphite.[3, 18] Marginal increases of the intensities of hydroxyl and carboxylate peaks for Al_2O_3-graphite as compared to the graphite may be ascribed to the heat treatment at 550 °C in air. Curve-fitting of the O1s spectra, as shown in Fig.8c, exhibits that the intensity of the peak at approximately 532.5 eV is obviously stronger than that at 533.8 eV in the spectrum of raw graphite, while in the spectrum of Al_2O_3-graphite, the latter is more remarkable conversely. Moreover, the ratio values between the intensities of the two peaks among the three spectra are in the order of Al_2O_3 < Al_2O_3-graphite < graphite. And we attributed these changes to the presence of alumina on the surface of graphite. Similar peaks of Al2p between Al_2O_3-graphite and alumina in Fig.8d further confirm that alumina nanoparticles were attached to the graphite surface successfully.

Journal Name

ARTICLE

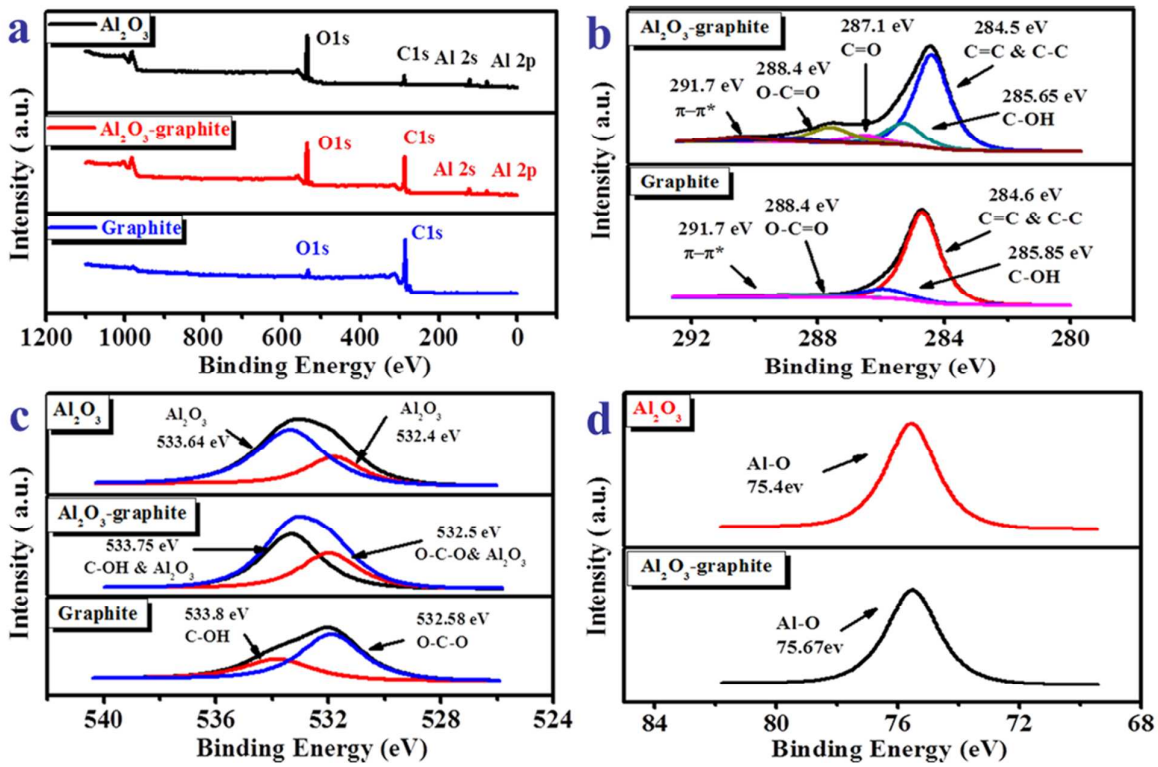

Fig. 8 XPS spectra of graphite, Al_2O_3-graphite, and Al_2O_3, (a) survey scans, (b) C1s, (c) O1s, and (d) Al2p.

Thermal conductivity and volume resistivity of epoxy composite

The thermal conductivity of polymer composite is related to the intrinsic thermal conductivity of filler and matrix as well as the type, size and loading content of fillers.[9, 42, 43] Fig.9 shows the variations in the thermal conductivities of various epoxy composites when different fillers and filler contents were used. It can be seen that slight improvements of the thermal conductivities of epoxy/Al_2O_3 composites could be observed in comparison with neat epoxy (0.22 W/mK) due to the low thermal conductivity of alumina.[21, 44] In contrast, both the thermal conductivities of epoxy/graphite and epoxy/Al_2O_3-graphite composites exhibit noticeable enhancements. This is basically because of the ultrahigh thermal conductivity of graphite and its flake shape facilitating the formation of thermal conductive chains. Additionally, epoxy/Al_2O_3-graphite composite shows lower thermal conductivity than the composite with raw graphite at high filler contents. For instance, with 18.4% filler loading, the thermal conductivities of the two composites are 0.76 and 0.64 W/mK, respectively. This reduction in the thermal conductivity values can be resulted from the following three reasons. Firstly, for the alumina-graphite fillers, alumina particles attached to the graphite surface lead to the decreasing amount of graphite in comparison to the neat graphite at a given filler content. As it is well known, graphite is the major component that enhances the thermal conductivities of epoxy composites.[3] Hence it is reasonable that the composite with lower amount of graphite would show lower thermal conductivity. Secondly, a comprehensive consistent idea has been accepted that the mode of thermal conduction in polymer is primarily phonons.[6, 7] Fig.6 shows that the thickness of alumina coating layer on the graphite surface is approximately 60.32 nm, which would retard the lateral movements of the phonons along the graphene sheets on graphite owing to the thermal conductivity difference of the two particles, namely 400 W/mK for graphite and 30 W/mK for alumina separately.[6] As a result, it would also lead to the reduction of thermal conductivity.[3] Thirdly, the thermal resistance is an important effect on the thermal conductivity of polymer composite.[1, 7, 12] For the epoxy/graphite composite, only one type of thermal resistance between graphite particles (graphite to graphite) exists compared with three types between alumina-coated graphite fillers (graphite to Al_2O_3, Al_2O_3 to Al_2O_3, and Al_2O_3 to graphite) for the epoxy/Al_2O_3-graphite composite,[3] as illustrated in Fig.10. As a consequence, greater thermal resistance between Al_2O_3-

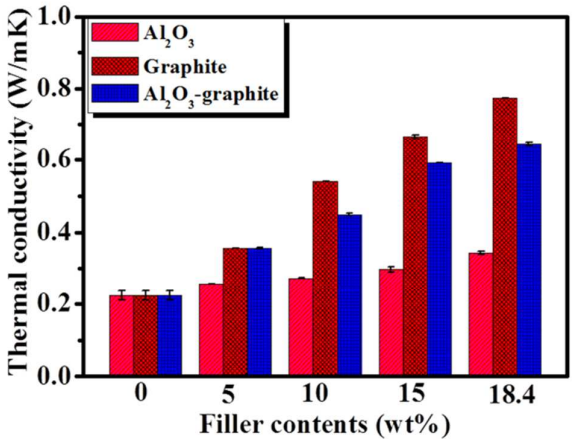

Fig. 9 Effect of various filler contents of Al_2O_3, graphite and Al_2O_3-graphite on the thermal conductivities of epoxy composites.

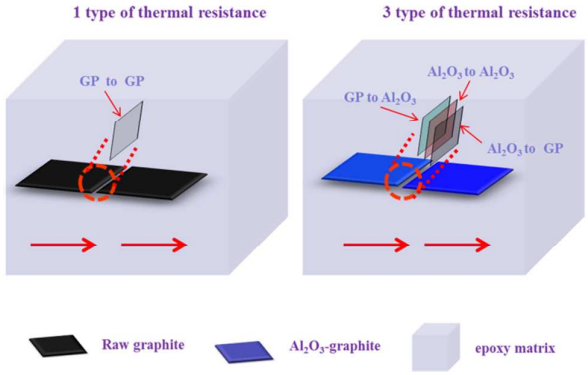

Fig. 10 Scheme of various in the thermal resistance of raw graphite and Al_2O_3-graphite in epoxy composites and the red line indicates the direction of thermal conduction (GP means graphite).

graphite particles would be obtained, inducing more retardation of thermal conduction, which would cause a lower thermal conductivity as well. Accordingly, those three factors contribute to the lower thermal conductivity of epoxy/alumina-coated graphite composite. However, the thermal conductivity of the coated composite in our report, 0.64 W/mK, still shows an obvious improvement compared to that of polymer/alumina-coated graphene composite, 0.45 W/mK, at a similar coated filler loading in a previous publication.[29] The difference may be attributed to the different coating methods.

Fig.11 shows the volume resistivity of as-prepared epoxy composites with various fillers as a function of filler loading. It is exhibited that adding alumina particles to the epoxy resin has very little effect on the electrical volume resistivity because of the intrinsic insulating property of that additive.[41] On the contrary, at raw graphite filler loading of 5%, the volume resistivity of composite decreases dramatically by about 7 orders of magnitude, from 1.91×10^{13} Ω cm for the neat epoxy to 1.58×10^{6} Ω cm. And with further addition of graphite particles, the volume resistivity of epoxy composite shows a very limited decline. For instance, the volume resistivity of epoxy/graphite composite with 18.4% filler loading is low to 3.1×10^{4} Ω cm. Overall, this indicates that an electrical percolating network is formed at a loading less than 5%,

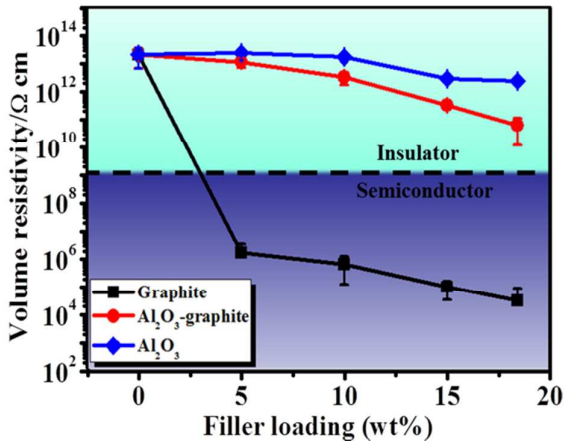

Fig. 11 Volume resistivity of epoxy composites containing various fillers and amounts of filler particles.

which corresponds well with some previous reports.[45, 46] This result is ascribed to the excellent electrical conductive property of graphite and its flake shape in favor of forming an efficient electrically conductive network.[3, 21, 30, 36] Modifying the graphite by applying the alumina coating layers significantly affects the electrical volume resistivity of epoxy composite. At low filler loadings (<10%), epoxy/Al_2O_3-graphite composites show almost the same volume resistivity as the neat epoxy. When the filler loading is up to 18.4%, the volume resistivity of the composite slightly decreases to 5.64×10^{10} Ω cm, which is three orders of magnitude lower than that of epoxy resin, suggesting this coated composite still could be regarded as an insulator.[21, 41] This phenomenon is resulted from the following reason. Electrically insulating alumina wrapping layer on the surface of graphite could keep each particle from coming into contact with each other, thus to increase the tunneling energy barrier and limit the inter-particles charge transport, which impedes the formation of electrically conductive network.[24, 36, 47] As a consequence, the epoxy/Al_2O_3-graphite composites still retain high electrical volume resistivity.

Microstructure of the epoxy composites

The microstructure of the fractured surfaces of the neat epoxy, epoxy/Al_2O_3, epoxy/graphite and epoxy/Al_2O_3-graphite composites was investigated by SEM method in Fig.12. It is shown in Fig.12a that the relatively smooth fracture surface of epoxy resin reveals a brittle fracture, while the fracture behaviors of epoxy composites have deviated from neat epoxy due to the addition of fillers. For the epoxy/Al_2O_3 composite, alumina particles are embedded in epoxy matrix in Fig.12b-c, indicating a strong interfacial bonding between resin and alumina due to the presence of polar groups (hydroxyl groups) on the alumina surface.[36] Fig.12d-e shows a few graphite particles were pulled out from the matrix, suggesting a weak matrix-filler interface of epoxy/graphite composite. In contrast, in Fig.12f-g, alumina-coated graphite particles could be well-embedded and uniformly dispersed in the epoxy matrix due to the improved interfacial interactions between fillers and matrix, which is ascribed to the Al_2O_3 layers exhibiting good miscibility with the epoxy resin.[29]

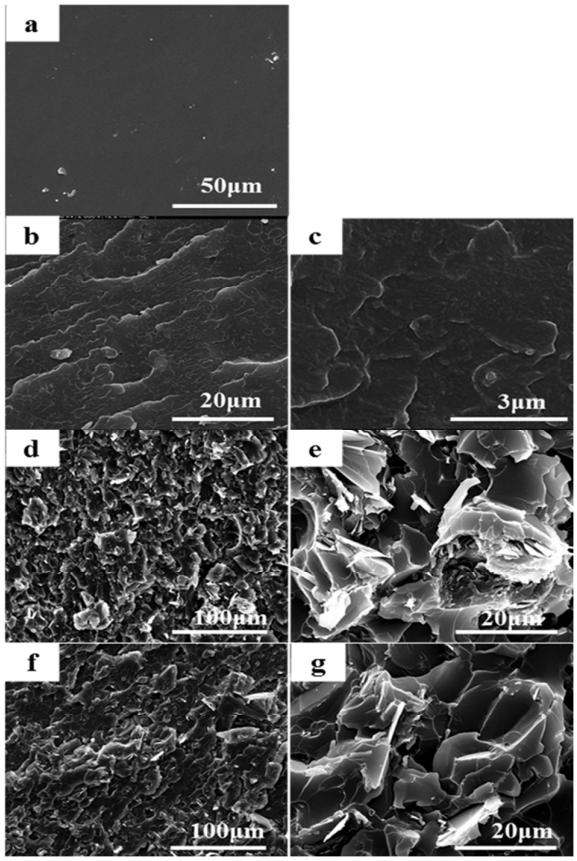

Fig. 12 SEM images of the fractured surface of neat epoxy (a), and the composites with 5 wt% fillers: alumina (b and c), raw graphite (d and e), and Al_2O_3-graphite (f and g).

Conclusions

In this study, uniform alumina coatings on graphite surface were successfully synthesized by a two-step coating method of chemical precipitation using aluminum nitrate as the coating precursor with the assistance of SDS surfactant and characterized by SEM, TEM, TGA and XPS methods. And the thickness of the homogenous coating layer is about 60.32 nm. A series of epoxy composites containing different coating or uncoating graphite fillers were prepared and compared. Though in comparison with the uncoated composites, the thermal conductivity of epoxy/Al_2O_3-graphite composite shows a moderate decrease, it still increases significantly to 0.64 W/mK from 0.22 W/mK for neat epoxy at the filler loading of 18.4%. However, the existence of insulating alumina layer could hinder the formation of a graphite electrically conductive network in epoxy matrix, resulting in retaining high volume resistivity (> $10^{10}\,\Omega$ cm) for epoxy/Al_2O_3-graphite composites when the coated filler is up to high contents. Our findings will be significant to provide some new guidance in developing thermal interface materials for potential application in thermal-control and electronic-packaging areas.

Acknowledgements

The authors are very grateful to the financial support from the National Science of China (51421061) and Sichuan Youth Science and Technology Foundation (2015JQ0012). And this work is also supported by the State Key Laboratory of Polymer Materials Engineering (Grant No. sklpme 2014-2-08).

Notes and references

College of Polymer Science and Engineering, the State Key Laboratory for Polymer Materials Engineering, Sichuan University, Chengdu 610065, PR China.
Email: yangqi@scu.edu.cn (Q. Yang).
Tel.: + 086 28 85401841; fax: + 086 28 85405402.

1 S. Ganguli, A. K. Roy and D. P. Anderson, *Carbon*, 2008, **46**, 806-817.
2 G. W. Lee, M. Park, J. Kim, J. I. Lee and H. G. Yoon, *Compos. Part A-Appl. S.*, 2006, **37**, 727-734.
3 S. Choi, K. Kim, J. Nam and S. E. Shim, *Carbon*, 2013, **60**, 254-265.
4 Z. Wang, T. Iizuka, M. Kozako, Y. Ohki and T. Tanaka, *Dielectrics and Electrical Insulation, IEEE Transactions on*, 2011, **18**, 1963-1972.
5 Y. Xu and D. Chung, *Compos. Interf.*, 2000, **7**, 243-256.
6 Z. Han and A. Fina, *Prog. Polym. Sci.*, 2011, **36**, 914-944.
7 J. Yu, X. Huang, C. Wu, X. Wu, G. Wang and P. Jiang, *Polymer*, 2012, **53**, 471-480.
8 K. Sato, H. Horibe, T. Shirai, Y. Hotta, H. Nakano, H. Nagai, K. Mitsuishi and K. Watari, *J. Mater. Chem.*, 2010, **20**, 2749-2752.
9 D. Tang, J. Su, M. Kong, Z. Zhao, Q. Yang, Y. Huang, X. Liao and Y. Niu, *Polym. Composite*, 2015.
10 W. Jiajun and Y. Xiao-Su, *Compos. Sci. Technol.*, 2004, **64**, 1623-1628.
11 Y. Xu, D. Chung and C. Mroz, *Compos. Part A-Appl. S.*, 2001, **32**, 1749-1757.
12 X. Huang, T. Iizuka, P. Jiang, Y. Ohki and T. Tanaka, *J. Phys. Chem. C*, 2012, **116**, 13629-13639.
13 T. Kusunose, T. Yagi, S. H. Firoz and T. Sekino, *J. Mater. Chem. A*, 2013, **1**, 3440-3445.
14 W. Zhou, C. Wang, T. Ai, K. Wu, F. Zhao and H. Gu, *Compos. Part A-Appl. S.*, 2009, **40**, 830-836.
15 Y. Noma, Y. Saga and N. Une, *Carbon*, 2014, **78**, 204-211.
16 J. G. Park, Q. Cheng, J. Lu, J. Bao, S. Li, Y. Tian, Z. Liang, C. Zhang and B. Wang, *Carbon*, 2012, **50**, 2083-2090.
17 C.-C. Teng, C.-C. M. Ma, C.-H. Lu, S.-Y. Yang, S.-H. Lee, M.-C. Hsiao, M.-Y. Yen, K.-C. Chiou and T.-M. Lee, *Carbon*, 2011, **49**, 5107-5116.
18 S.-Y. Yang, W.-N. Lin, Y.-L. Huang, H.-W. Tien, J.-Y. Wang, C.-C. M. Ma, S.-M. Li and Y.-S. Wang, *Carbon*, 2011, **49**, 793-803.
19 F. H. Gojny, M. H. Wichmann, B. Fiedler, I. A. Kinloch, W. Bauhofer, A. H. Windle and K. Schulte, *Polymer*, 2006, **47**, 2036-2045.
20 N. Shenogina, S. Shenogin, L. Xue and P. Keblinski, *Appl. Phys. Lett.*, 2005, **87**, 133106.
21 X. Pu, H.-B. Zhang, X. Li, C. Gui and Z.-Z. Yu, *RSC Adv.*, 2014, **4**, 15297-15303.
22 Y. S. Song and J. R. Youn, *Carbon*, 2005, **43**, 1378-1385.
23 I. Krupa, I. Novák and I. Chodák, *Synthetic Met.*, 2004, **145**, 245-252.
24 W. Cui, F. Du, J. Zhao, W. Zhang, Y. Yang, X. Xie and Y.-W. Mai, *Carbon*, 2011, **49**, 495-500.
25 J. Zhao, F. Du, W. Cui, P. Zhu, X. Zhou and X. Xie, *Compos. Part A-Appl. S.*, 2014, **58**, 1-6.

26 S. Choi, Y. Kim, J. H. Yun, I. Kim and S. E. Shim, *Mater. Let.t*, 2013, **90**, 87-89.
27 T. D. Dao, H.-i. Lee and H. M. Jeong, *J. Colloid Interface Sci.*, 2014, **416**, 38-43.
28 K. T. Kim, T. D. Dao, H. M. Jeong, R. V. Anjanapura and T. M. Aminabhavi, *Mater. Chem. Phys.*, 2015,**153**, 291-300.
29 R. Qian, J. Yu, C. Wu, X. Zhai and P. Jiang, *RSC Adv.*, 2013, **3**, 17373-17379.
30 Y. Zhang, S. Xiao, Q. Wang, S. Liu, Z. Qiao, Z. Chi, J. Xu and J. Economy, *J. Mater. Chem.*, 2011, **21**, 14563-14568.
31 Q. Yang, Y. Deng and W. Hu, *Ceram Int*, 2009, **35**, 1305-1310.
32 H. Jin, Z. Ji, Y. Li, M. Liu, J. Yuan, C. Xu and S. Hou, *Colloid. Surface. A*, 2014, **441**, 170-177.
33 K. Kawabata, H. Yoshimatsu, E. Fujii, K. Hiragushi, A. Osaka and Y. Miura, *J. Mater. Sci. Let.t*, 2001, **20**, 851-853.
34 S. Yilmaz, Y. Kutmen-Kalpakli and E. Yilmaz, *Ceram. Int.*, 2009, **35**, 2029-2034.
35 Y.-H. Li, S. Wang, A. Cao, D. Zhao, X. Zhang, C. Xu, Z. Luan, D. Ruan, J. Liang and D. Wu, *Chem. Phys. Lett.*, 2001, **350**, 412-416.
36 S. Choi, J. Yang, Y. Kim, J. Nam, K. Kim and S. E. Shim, *Compos. Sci. Technol.*, 2014, **103**, 8-15.
37 E. Verwey, *J. Phys. Chem.*, 1947, **51**, 631-636.
38 Y. Yang, S. Qiu, W. Cui, Q. Zhao, X. Cheng, R. K. Y. Li, X. Xie and Y.-W. Mai, *J. Mater. Sci.*, 2009, **44**, 4539-4545.
39 B. Cheng, L. Zhao, J. Yu and X. Zhao, *Mater Res Bull*, 2008, **43**, 714-722.
40 J. Guo, P. Saha, J. Liang, M. Saha and B. P. Grady, *J. Therm. Anal. Calorim.*, 2013, **113**, 467-474.
41 M.-C. Hsiao, C.-C. M. Ma, J.-C. Chiang, K.-K. Ho, T.-Y. Chou, X. Xie, C.-H. Tsai, L.-H. Chang and C.-K. Hsieh, *Nanoscale*, 2013, **5**, 5863-5871.
42 W. Zhou, S. Qi, Q. An, H. Zhao and N. Liu, *Mater. Res. Bull.*, 2007, **42**, 1863-1873.
43 Y. X. Fu, Z. X. He, D. C. Mo and S. S. Lu, *Appl. Therm. Eng.*, 2014, **66**, 493-498.
44 Y. Okazaki, M. Kozako, M. Hikita and T. Tanaka, Solid Dielectrics (ICSD)**,**10th IEEE International Conference on, IEEE, Germany, 2010, pp. 1-4.
45 W. Zheng and S.-C. Wong, *Compos. Sci. Technol.*, 2003, **63**, 225-235.
46 G. Chen, W. Weng, D. Wu and C. Wu, *Eur. Polym. J.*, 2003, **39**, 2329-2335.
47 F. M. Blighe, Y. R. Hernandez, W. J. Blau and J. N. Coleman, *Adv. Mater.*, 2007, **19**, 4443-4447.